THE ASTROPHYSICAL JOURNAL, 260:512–519, 1982 September 15

APPARENT PROPER MOTIONS OF THE GALACTIC CENTER COMPACT RADIO SOURCE AND PSR 1929+10

D. C. BACKER
Radio Astronomy Laboratory, University of California at Berkeley
AND
R. A. SRAMEK
National Radio Astronomy Observatory
Received 1982 January 22; accepted 1982 March 31

ABSTRACT

The techniques of differential radio astrometry with a connected-element interferometer are presented. The motion of the compact, nonthermal radio source in the galactic center is found to be consistent with the secular parallax expected for an object at rest in the galactic center. The proper motion of PSR 1929+10 has been improved, and new limits on its trigonometric parallax are determined.

Subject headings: galaxies: Milky Way — galaxies: nuclei — pulsars

I. INTRODUCTION

Differential radio astrometry with microwave interferometers has the potential for measuring many quantities of astronomical interest: proper motion and trigonometric parallaxes of pulsars, orbital parameters of compact galactic radio stars located in binary systems, kinematics of objects in the galactic center (including the secular parallax arising from galactic rotation), proper motions of the centroids of violently variable extragalactic sources, and gravitational deflection of electromagnetic radiation by the Sun. At the present time, only a few of these tasks have been accomplished. The central problems have been both instrumental and human: sensitive long-baseline ($\gtrsim 10^6\ \lambda$) interferometers with astrometric capability have been constructed only in the last decade, and great persistence is required to obtain and to analyze the necessary series of observations.

The 35 km Green Bank interferometer, operated until 1979 by the National Radio Astronomy Observatory[1] and since 1979 by the US Naval Observatory, has provided new opportunities to perform the aforementioned experiments. We have reported previously our first results on pulsar proper motions (Backer and Sramek 1976, hereafter Paper I; 1981). The use of the instrument to measure gravitational deflection has been described by one of us (Fomalont and Sramek 1975). In this paper, we expand on the description of our differential astrometric techniques contained in Paper I with particular attention to analysis of errors. Then we present two results from this program. Our measurements of the apparent position of the compact, nonthermal radio source in the galactic center, Sgr A(cn), are consistent with the secular parallax arising from rotation of the Galaxy and set a limit on one component of its peculiar motion. Our determination of the proper motion and trigonometric parallax of pulsar 1929+10 is compared with the values obtained both by previous interferometer programs and by the pulse-timing technique.

[1]The National Radio Astronomy Observatory is operated by Associated Universities, Inc., under contract with the National Science Foundation.

II. METHOD

The use of the Green Bank interferometer for differential astrometry has been described in Paper I and by Fomalont and Sramek (1975). The observations proceeded in three stages: recording at the telescope, correction for *a priori* effects, and analysis for differential position and proper motion. In this section, we will present the phase data model used in various stages of processing.

For our experiment we used only the three 35 km baselines formed by the four-element Green Bank interferometer. The observable containing source position information for each pair of antennas is the interferometer phase

$$\phi(\lambda, s, t) = \boldsymbol{b}(\lambda, t)\cdot\boldsymbol{s} + k\cos\delta + \phi_p(\boldsymbol{s}, \boldsymbol{b}, t) + \phi_n(t) + \phi_s(h) + \phi_c(t), \quad (1)$$

where $\boldsymbol{b} = (b_x \cos\Omega t + b_y \sin\Omega t,\ b_x \sin\Omega t - b_y \cos\Omega t,\ b_z)$ is the baseline vector which moves as a consequence

TABLE 1

ACCURACY OF PHASE MODEL IN DIFFERENT PROCESSING STEPS

Parameter	Telescope	Correction	Difference
Precession	0.01	0.01	< 0.001[a]
Position (1950)	0.2–10	3	0.3
Baseline	1	0.1	≤ 0.005
Sidereal time	1.5	0.03	< 0.001[b]
Propagation:			
Troposphere[c]	0.5	0.2	≤ 0.010
Ionosphere[c]	0.02	0.02	< 0.001
Gravitational deflection	$\ll 1$	$\ll 1$	< 0.001[d]

NOTE.—All entries are in wavelengths at 2.7 GHz or, equivalently, arc seconds.

[a] Precession error during Epoch V at telescope was removed.

[b] Sidereal time error in edit step for Epoch XII was removed.

[c] These terms increase with secant of zenith angle.

[d] Only significant error occurred for Sgr A(cn) during Epoch VII.

of Earth rotation (Ω); $s = (\cos\alpha\cos\delta, \sin\alpha\cos\delta, \sin\delta)$ is a unit vector toward a radio source in a quasi-inertial[2] frame of reference; k is a constant which accounts for the difference in the separation of the polar and declination axes of the two antennas; ϕ_p is the phase difference resulting from propagation delays from the radio source to the two antennas; ϕ_n is the random noise; ϕ_s is the consequence either of asymmetric structure in the observed sources or of background sources in the field of view and is dependent on the hour angle $h = t - \alpha$; ϕ_c is the electrical collimation which varies slowly with time; and t is the local sidereal time. In equation (1) and below, phase is measured in cycles, and baselines are given in wavelengths of the standard observing frequency 2695 MHz.

The accuracy of the phase model at various stages of data reduction is summarized in Table 1. The second column in Table 1 gives the model accuracy at the telescope. The propagation term is unmodeled, and a smooth approximation to local sidereal time is used. Slow variations of the actual center frequency of the instrument are monitored for later correction. The residual phases from the model for the three baselines with two polarizations are recorded on magnetic tape for a 4 hr observing sequence of: reference 1 - reference 2 - program object - ref 1 - obj - ref 2...ref 1 - ref 2. The typical interval between object observations is 10–20 minutes. Separations between object and reference sources are typically 0.1 rad or less.

The third column in Table 1 lists estimated errors after applying five corrections to the telescope phases using standard NRAO/USNO software. (1) Errors in the assumed 1950.0 positions are removed based on information obtained after the initiation of the program. (2) Baselines were corrected to values determined by NRAO/USNO personnel. The new values included effects of the variable spin parameters of the Earth and Earth tides at the time of their determination. At the epoch of our observations, the accuracy will have been degraded slightly. (For example, polar motion is $\sim 0''.1$ month^{-1}.) The phase was corrected both (3) for drifts in the actual center frequency from the nominal value and (4) for the error in the approximate sidereal time used at the telescope. (5) A bi-exponential model of the troposphere was removed according to

$$\phi_t = A(\eta_W + \eta_D)\sec z + (\boldsymbol{b}_0 \cdot \boldsymbol{s}_0) \times \left(\eta_W h_W e^{-A/h_W} + \eta_D h_D e^{-A/h_D}\right)\sec^2 z/R. \quad (2)$$

In equation (2), η_W, η_D and h_W, h_D are the refractivities and scale lengths for the wet and dry components of the atmosphere, respectively, A is the altitude difference between the antennas, and R is the radius of the Earth. The refractivities were computed using average pressure, temperature, and dew point measurements obtained from weather stations near the control room and at the remote site. Scale heights of 9.0 and 2.5 km for the dry and wet terms, respectively, were used for all epochs. Typical zenith corrections are 0.5 λ for the altitude difference term and 0.15 λ for the spherical Earth term. Errors in the model and from a difference in weather between the local and remote sites probably do not exceed 0.2 λ for high-elevation observations.

The propagation phase in equation (1) will also contain differential retardation of the ionosphere. We have not attempted to model this effect since we had no ionospheric monitor. Komesaroff (1960) has shown that

[2] We use the term *quasi-inertial* because we explicitly recognize the diurnal motion of the baseline, not the sources. However, we do update the source positions during each observation for precession, nutation, and aberration, not the baseline. Other secular irregularities in the Earth's spin are incorporated into the baseline vector determination each epoch.

at a zenith angle of 45°, typical refraction angles for a spherical ionosphere at 20 MHz are 1°. The refraction angles at 2.7 GHz would be 3″ using a ν^{-2} scaling. We approximate that typical errors from ionospheric propagation are 0.″02 for high-elevation observations since the zenith angle difference between our antennas is $|\boldsymbol{b}|/R \approx 0.005$. This error term has diurnal, seasonal, and random variations of nearly 100%. In particular, Komesaroff suggests that "wedge" refraction resulting from diurnal and latitudinal variations has a magnitude comparable to the spherical value.

The phase residual, observed minus model, after the corrections contained in the NRAO/USNO standard programs may be represented as

$$\phi_r(\boldsymbol{s}_i, t_j) = \boldsymbol{b}_0(t_j) \cdot \Delta \boldsymbol{s}_i + \Delta\phi_p(\boldsymbol{s}_i, \boldsymbol{b}, t_j) + \phi_n(t_j) + \phi_c(t_j) + O(0.1) \quad (3)$$

for each source at $\boldsymbol{s}_i$ and for each observation at t_j. The final term in equation (3) represents a collection of small terms remaining from equation (1). These residual phases, and the corresponding amplitudes, are written on magnetic tape and brought to Berkeley, where the phase differencing and final analysis are done.

In the differencing step the reference source phases are interpolated in time to the times of the adjacent object scans. A weighted mean of the interpolated reference source phases is subtracted from the object source phase to form a difference phase

$$\Phi(\boldsymbol{s}, t_j) = \phi_r(\boldsymbol{s}, t_j) - \sum_{i=1}^{2} w_i \phi_r(\boldsymbol{s}_i, t_j). \quad (4)$$

The weighted average of our two reference source positions is called the *pseudo–reference source* position and is typically 0.02 rad from the object position. The second and third terms of equation (3) may be Taylor expanded about the object source position and observing times. The linear terms in angle and in time dominate the expansion. The differencing removes these leading terms from the object residual phases, thereby reducing the phase errors by 0.02, as tabulated in the fourth column of Table 1.

The difference phase for each epoch, T, may be modeled as

$$\Phi(\boldsymbol{s}, t_j, T) = \boldsymbol{b}_0(t_j, T) \cdot \Delta \boldsymbol{s}_{\rm pp}(T) + \text{noise}. \quad (5)$$

In equation (5), $\Delta \boldsymbol{s}_{\rm pp}$ is the *pseudo–position offset* which we determine for each epoch from a least-squares fit to Φ over the t_j using a baseline for that epoch accurate to 1 λ and using the apparent position of the program object, $\boldsymbol{s}$. Pseudo–position offsets are determined for each channel on each day of a given epoch. Since our UV coverage is limited, the errors in α and δ from the fit for $\Delta \boldsymbol{s}_{\rm pp}$ are highly correlated. Following the work of Brosche, Wade, and Hjellming (1973), we determine the principal axes of the error ellipse and rotate $\Delta \boldsymbol{s}_{\rm pp}$ to these axes. The offsets and their errors, the date, and the position angle of the new coordinate system from each fit are stored for final analysis.

From equations (3) and (4) we can see that the pseudo–position offsets for any program object will contain both a constant of order 0.″3 resulting from imprecise determination of the absolute positions of all sources in a sequence and a varying term arising from proper motion ($\boldsymbol{\mu}$), and perhaps annual parallax ($\boldsymbol{\pi}$), and secular parallax ($\boldsymbol{P}$):

$$\Delta \boldsymbol{s}_{\rm pp}(T) = \Delta \boldsymbol{s}_{\rm obj}(T_0) - \sum_{i=1}^{2} W_i \Delta \boldsymbol{s}_{\rm ref}(i) + \boldsymbol{\mu}\Delta T + \boldsymbol{\pi}(T) + \boldsymbol{P}\Delta T. \quad (6)$$

In our final analysis step, we consider all pseudo–position offsets from all epochs. Data which are obviously spurious are edited, and each offset is rotated to a single coordinate system with the average postion angle; differences of ±1° between the principal axes exist for the different baseline channels and for observing days foreshortened owing to scheduling or to equipment failure. The differential gravitational deflection of electromagnetic radiation by the Sun is then removed from all offsets. This effect was as large as 0.″03 for our Sgr A(cn) observation in 1976 December.

The edited and corrected offsets are then averaged for each epoch. If desired, weights equal to the inverse of the variance from the fit are used in computing the mean. The error in the epoch-average offset is the observed standard deviation of the N values entering the average reduced by $(N/2)^{1/2}$. The factor of 2 is somewhat arbitrary but does account both for the correlation of offsets determined from two polarization channels on the same baseline and for the correlation of the propagation phase between all channels. The reduction in N is not taken to be greater than 2 since we are dealing with faint radio sources with significant random noise.

The epoch-average offsets are fit by least squares to a constant and a proper motion along each axis.

III. RESULTS

We describe below results from our differential astrometry program for the galactic center source and for PSR 1929+10. Proper motions for other pulsars have been presented elsewhere (Backer and Sramek 1981). A journal of the observations is presented in Table 2.

a) Galactic Center Source

We added the compact, nonthermal object in the galactic center, Sgr A(cn), to our differential astrometry

TABLE 2

JOURNAL OF OBSERVATIONS

Epoch	Julian Date (2,440,000.+)	Calendar Date	Group I PSRs[a]	Group II PSRs[b]	Sgr A(cn)
I	2176.	1974 May	×	...	...
II	2350.	1974 Oct	×	...	...
III	2494.	1975 Mar	×	...	...
IV	2742.	1975 Nov	×	...	...
V	2878.	1976 Apr	×	×	×
VI	3054.	1976 Oct	×	×	×
VII	3129.	1976 Dec	...	...	×
VIII	3227.	1977 Mar	...	...	×
IX	3305.	1977 Jun	...	...	×
X	3395.	1977 Sep	...	...	×
XI	3528.	1978 Jan	×	×	×
XII	4343.	1980 Apr	...	...	×
XIII	4701.	1981 Apr	...	...	×

[a]Group I: 0329+54, 0950+08, 1133+16, 1929+10, 2021+51.
[b]Group II: 0355+54, 0950+08, 2020+28.

program in Epoch IV, 1975 November, soon after the object was definitively observed by Balick and Brown (1974). We hope to obtain sufficient accuracy in these observations to detect the galactic rotation as a secular parallax of Sgr A(cn) viewed relative to an (assumed) extragalactic frame. Any peculiar motion of Sgr A(cn) relative to the expected secular parallax would provide a mass estimate for this enigmatic object. Current models favor both high masses (Lynden-Bell and Rees 1971; Oort 1977) and low masses (Reynolds and McKee 1980).

The secular parallax for an object in the galactic center consists of the difference between Oort's con-

TABLE 3

ASTROMETRIC PARAMETERS FOR SGR A(CN) OBSERVATIONS

A. POSITIONS

Source	R.A. (1950.0) h	m	s	Decl. (1950.0) °	′	″	Weight
35 km/11 cm							
Sgr A(cn) ...	17	42	29.291	−28	59	17.63	...
1741−312 ...	17	41	09.32	−31	15	20.4	0.63
1748−253 ...	17	48	45.79	−25	23	17.7	0.37
VLA/6 cm							
Sgr A(cn) ...	17	42	29.319	−28	59	18.54	...
1741−312 ...	17	41	09.340	−31	15	21.00	...
1748−253 ...	17	48	45.792	−25	23	17.74	...

B. APPARENT PROPER MOTION (″ yr^{-1})

Weighting	x-Component (P.A. = 136°)	x-Error	y-Component (P.A. = 46°)	y-Error
A-uniform[a] ...	+0.0077	0.0250	−0.0061	0.0024
B-variance[b] ...	−0.0104	0.0190	−0.0075	0.0023
Average	−0.0014	0.0220	−0.0068	0.0024

[a]Equal weight given to each epoch.
[b]Weight for each epoch proportional to inverse of variance from intraepoch average.

stants, $A-B$, and the peculiar solar motion. In galactic coordinates, the expected secular parallax is

$$P_l = -(A-B) - \dot{Y}_\odot / R_\odot ,$$

$$P_b = -\dot{Z}_\odot / R_\odot . \qquad (7)$$

These motions are

$$P_l = -0''.0056 \text{ yr}^{-1},$$

$$P_b = -0''.0002 \text{ yr}^{-1}, \qquad (8)$$

with

$$(A-B) = 250 \text{ km s}^{-1}/10 \text{ kpc},$$

$$\dot{Y}_\odot = 15.3 \text{ km s}^{-1},$$

$$\dot{Z}_\odot = 7.4 \text{ km s}^{-1},$$

$$R_\odot = 10 \text{ kpc}$$

from Allen (1973).

Two compact reference sources near Sgr A(cn) were found in the survey of Clark and Crawford (1974). Their positions, measured with the 35 km interferometer, and the weights used in our analysis are given in Table 3A along with the assumed position for Sgr A(cn) (Balick and Brown 1974). We also list for future reference improved coordinates for the three sources from 6 cm VLA observations. We assume that the reference sources are extragalactic. Our principal arguments for their extragalactic nature are that their brightness temperatures exceed 10^{10} K (unpublished VLBI observations) and that their variability time scales exceed 1 yr. Apart from Sgr A(cn), the only galactic objects with comparable brightness temperatures are binary radio stars which vary with time scales of days (e.g., Cyg X-3, Algol).

Phase residuals (eq. [3]) for the three sources from one correlator channel are displayed in Figure 1 for 6 days to illustrate the difficulties associated with astrometric observations. During Epoch V there was a 1 day precession error which resulted in the phase drift in Figure 1. The large dip in the Epoch VI observations probably was the result of a tropospheric delay correlated over the Sgr A(cn)–reference sources angular field. The Epoch VII measurements were obtained in mid-December when 1748−253 was only 5° from the Sun; the large fluctuations are probably the effect of turbulence in the solar corona. Measurements at 8 GHz were simultaneously recorded during Epochs VI, VII, and XIII. The higher frequency measurements were difficult to analyze owing to rapid tropospheric phase variations.

Pseudo–position offsets for Sgr A(cn) are given in Figure 2 along with two least-squares fits for proper motion components. The measurements are most accurate for a position angle (P.A.) of 46°, the mean projection of the baseline. This principal axis, the y-axis, nearly parallels the galactic plane at P.A. of 32°. Two solutions for proper motion using different weighting schemes are plotted in Figure 2 and listed in Table 3B: solution A, uniform weight to each epoch, and solution B, weight proportional to the inverse of the variance for each intraepoch average. The 8 GHz measurements are shown with crosses on Figure 2. The consistency of the pseudo–position offsets for the two frequencies indicates our insensitivity to ionospheric errors.

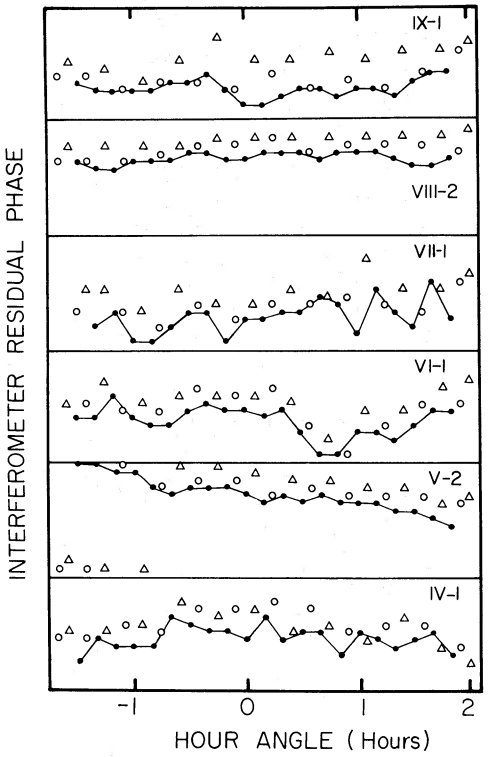

FIG. 1.—Residual interferometer phases for Sgr A(cn) (*filled circles*) and two reference sources (*open circles* = 1741−312; *triangles* = 1748−253) after corrections with the NRAO software. Baseline is between fixed antenna 1 and the remote site. In each box the epoch and day are given in the upper right. The height of each box corresponds to one turn of phase at 11 cm, or ~1″.

The average of the two proper motion fits,

$$\mu_x = -0''.0014 \pm 0''.0220 \text{ yr}^{-1},$$

$$\mu_y = -0''.0068 \pm 0''.0024 \text{ yr}^{-1}, \qquad (9a)$$

agrees well with the secular parallax computed above projected into the (x, y)-coordinate system:

$$P_x = +0''.0016 \text{ yr}^{-1},$$

$$P_y = -0''.0054 \text{ yr}^{-1}. \qquad (9b)$$

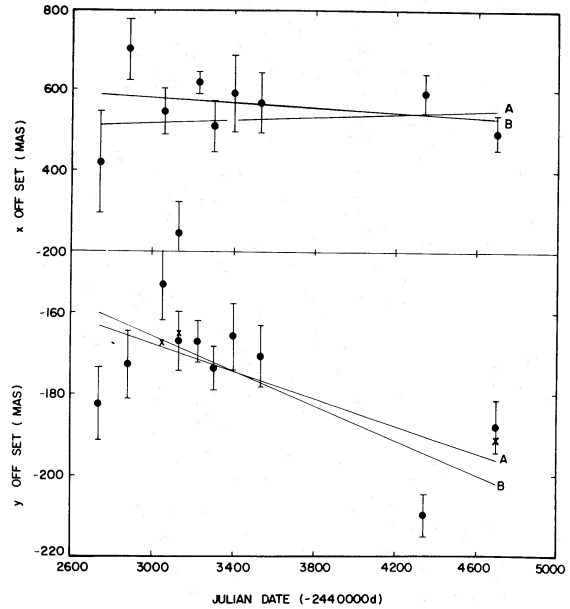

FIG. 2.—Pseudo–position offsets for Sgr A(cn) along axes at P.A. = 136°.0 (x-axis) and 46°.0 (y-axis). The position angle of the galactic plane is 31°.8. Two fits for proper motion components in x and y are given; fit A weights all measurements uniformly, while fit B weights measurements by the inverse of their variances. The crosses ("X") denote pseudo–position offsets measured simultaneously at X band ($\lambda = 3.7$ cm). The y-component proper motions correspond to velocities of 290 ("A") and 360 ("B") km s^{-1} at a distance of 10 kpc.

The residual motion in the y-coordinate, $\mu_y - P_y$, corresponds to -65 ± 100 km s^{-1}. The 3 σ limit for the peculiar motion in y is 300 km s^{-1}. The present accuracy does not allow a discussion of either the object's mass or the accuracy of the galactic constants. The measurement does confirm that Sgr A(cn) is at the galactic center and is not a chance background extragalactic object. Further observations are in progress using the VLA which will provide improved accuracy, as well as two-coordinate coverage. The 35 km program will be continued until superseded by the VLA measurements.

b) PSR 1929+10

The proper motion of 1929+10 was found to be $\sim 0''.1$ yr^{-1} during the first 2 yr of this program (Paper I). More recently the proper motion has been determined by Helfand *et al.* (1980) and by Gullahorn and Rankin (1978*a*, *b*) using the pulse-timing technique. These three measurements disagree with each other. We have reanalyzed all of our observations with the revised software described in the preceding section. An error was found in the analysis software used in Paper I which had a serious effect on the right ascension motions. All objects in Paper I would be affected in a similar way. Final proper motions from this program both for the five objects in Paper I and for PSR 0355+54 and PSR 2020+28 are tabulated in Backer and Sramek (1981).

In the 1929+10 observations, we used two reference sources located to the southeast and southwest. The coordinates of these sources are given in Table 4A along with the weights used to form the pseudo–reference source residual phase. The absolute accuracy of these coordinates is $\sim 0''.2$.

In Figure 3 we present pseudo–position offsets of 1929+10 in a left-hand coordinate system in which the minimum errors occur along the y-axis. The y-axis is oriented at P.A. 40°.6. The measurements from Epoch I (JD 2,442,176) are shown without errors and were not included in the fit described below, since only a few correlators were operating correctly for pulsar signals. The errors for each epoch are determined from the internal consistency of the data from the three baselines.

TABLE 4

ASTROMETRIC PARAMETERS FOR PSR 1929+10 OBSERVATION

A. POSITIONS

SOURCE	R.A. (1950.0) h	m	s	DECL. (1950.0) °	′	″	WEIGHT
Pulsar	19	29	51.93[a]	10	53	03.8[a]	...
Reference 1 ...	19	15	22.10	6	15	55.6	0.445
Reference 2 ...	19	47	40.17	7	59	34.9	0.555

B. APPARENT PROPER MOTION (″ yr^{-1})

x-Component (P.A. = 130°.6)	x-Error	y-Component (P.A. = 40°.6)	y-Error
0.0010	0.0300	0.0701	0.0025

[a]These positions are for epoch 1975.5 for the proper motion expressed in the coordinate system of 1950.0.

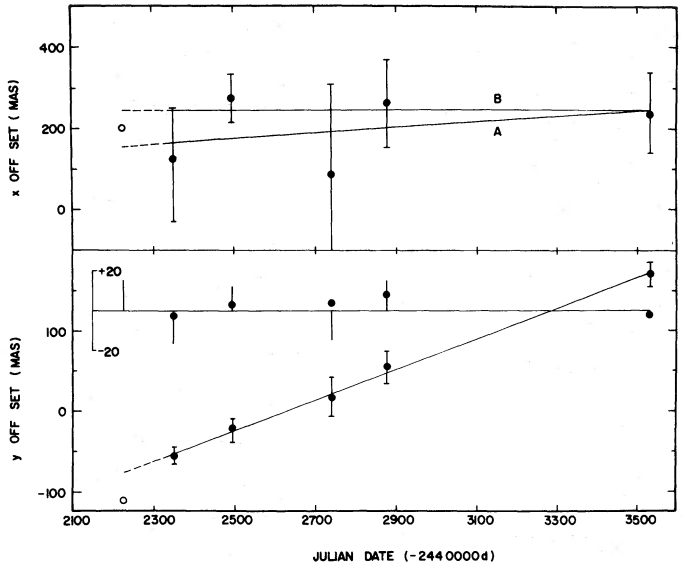

FIG. 3.—Pseudo–position offsets for PSR 1929+10 along axes at P.A. 130°6 (x-axis) and 40°6 (y-axis). Solid lines show results of least-squares fits for proper motion in x and in y. The two lines marked "A" and "B" correspond to fits with uniform and error-dependent weights. The errors are determined from the variance of individual measurements for each epoch. The residuals from the y proper motion fit are shown relative to a horizontal line along with vertical bars which indicate the expected residuals for the 0".02 trigonometric parallax of Salter, Lyne, and Anderson (1979).

This procedure overestimates the y-errors owing to a small and constant difference for all epochs between the y-offsets for the three baselines. We attribute the differences to structure in one of the reference sources. The results of a weighted least-squares fit to the measurements are tabulated in Table 4B and plotted in Figure 3.

Included in Figure 3 are the expected residuals from a linear fit to the y-offsets resulting from the 0".02 trigonometric parallax reported by Salter, Lyne, and Anderson (1979). Our residuals indicate a much smaller parallax of 0".004 which, to be consistent with the dispersion measure, requires a mean electron density of 0.013 cm^{-3} along the 250 pc path to 1929+10.

We present in Figure 4 a comparison of our new proper motion with the timing results mentioned above. The agreement with Helfand *et al.* (1980) is satisfactory. These results disagree with the nominally more accurate values of Gullahorn and Rankin (1978*a*, *b*). Our new results indicate a motion primarily in galactic longitude. The apparent approach of this pulsar toward the galactic plane, which we reported in Paper I, was a result of the program error discussed above. At a distance of 250 pc, the projected motion of 1929+10 is ~85 km s^{-1} parallel to the plane and ~25 km s^{-1} perpendicular to the plane. If 1929+10 were at 50 pc, then its space velocity would be 18 km s^{-1}, much smaller than the typical transverse velocity of 145 km s^{-1} (Lyne 1981).

IV. CONCLUSION

The accuracy obtainable in differential radio astrometry programs on faint galactic objects is ~ $0''.01/T$ yr^{-1}

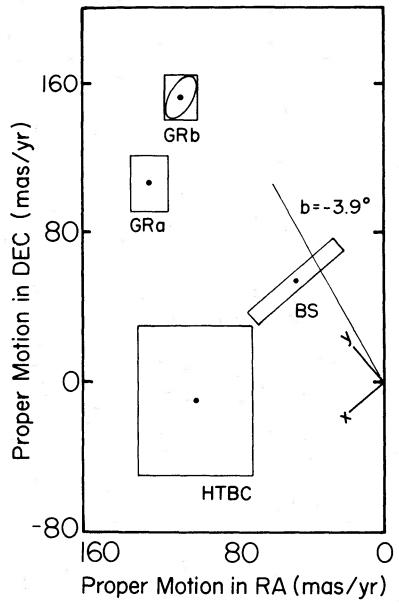

FIG. 4.—Comparison of proper motions from radio interferometry and from timing analyses. The boxes labeled "GR" and "HTBC" are from Gullahorn and Rankin (1978*a*, *b*) and from Helfand *et al.* (1980). The interferometer result presented in this paper is labeled "BS." The axis labeled $b = -3°.9$ is parallel to the galactic plane at negative latitude 3°.9.

with a baseline of $3\times10^5\,\lambda$, where T is the time range of the observations in years. We have determined with this accuracy the proper motion of PSR 1929+10 and have set a new limit of 0".004 on its trigonometric parallax. Measurements of the galactic center compact radio source are consistent with the secular parallax expected for an object nearly at rest in the center of the Galaxy.

The VLA will provide new opportunities for differential astrometry on galactic objects. The larger effective aperture and lower noise receivers provide an increase in the sensitivity which, in turn, allows measurements with closer, fainter reference sources. Improvements in modeling the troposphere, a major error source in the present work, will also reduce the uncertainty in future work. Motions less than 0".001 yr^{-1} should be observable with connected-element interferometers.

We are grateful to the interferometer staff at Green Bank for their diligent assistance and to NRAO, Cornell University, GSFC, and the University of California for their support during the execution of this program. We thank also the USNO for allowing the continuation of the Sgr A(cn) observations.

REFERENCES

Allen, C. W. 1973, *Astrophysical Quantities* (London: Athlone Press).
Backer, D. C., and Sramek, R. S. 1976, *A.J.*, **81**, 430 (Paper I).
_____. 1981, in *IAU Symposium 95, Pulsars*, ed. W. Sieber and R. Wielebinski (Dordrecht: Reidel), p. 205.
Balick, B., and Brown, R. L. 1974, *Ap. J.*, **194**, 265.
Brosche, P., Wade, C. M., and Hjellming, R. M. 1973, *Ap. J.*, **183**, 805.
Clark, D. H., and Crawford, D. F. 1974, *Australian J. Phys.*, **27**, 713.
Fomalont, E. B., and Sramek, R. A. 1975, *Ap. J.*, **199**, 749.
Gullahorn, G. E., and Rankin, J. M. 1978*a*, *A.J.*, **83**, 1219.
_____. 1978*b*, *Ap. J.*, **225**, 963.
Helfand, D. J., Taylor, J. H., Backus, P. B., and Cordes, J. M. 1980, *Ap. J.*, **237**, 206.
Komesaroff, M. M. 1960, *Australian J. Phys.*, **13**, 153.
Lynden-Bell, D., and Rees, M. J. 1971, *M.N.R.A.S.*, **152**, 461.
Lyne, A. G. 1981, in *IAU Symposium 95, Pulsars*, ed. W. Sieber and R. Wielebinski (Dordrecht: Reidel), p. 423.
Oort, J. H. 1977, *Ann. Rev. Astr. Ap.*, **15**, 295.
Reynolds, S. P., and McKee, C. F. 1980, *Ap. J.*, **239**, 893.
Salter, M. J., Lyne, A. G., and Anderson, B. 1979, *Nature*, **280**, 477.

D. C. Backer: Radio Astronomy Laboratory, 601 Campbell Hall, University of California, Berkeley, CA 94720

R. A. Sramek: Very Large Array, National Radio Astronomy Observatory, P.O. Box O, Socorro, NM 87801